Crystallization of Poly(ethylene oxide) Patterned by Nanoimprint Lithography

Brian C. Okerberg,[†] **Christopher L. Soles,*** **Jack F. Douglas, Hyun Wook Ro, and Alamgir Karim**

Polymers Division, National Institute of Standards and Technology, 100 Bureau Drive, Gaithersburg, Maryland 20899-8541

Daniel R. Hines

Laboratory for Physical Sciences, University of Maryland, 8050 Greenmead Drive, College Park, Maryland 20740
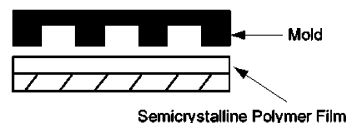
Crystallization of polymeric materials in confined geometries is a subject of intense recent interest. It has been shown that confinement of semicrystalline polymers in thin films can significantly affect primary nucleation, the crystal morphology, crystal growth rates, and the crystal orientation.[1−10] Nanoimprint lithography (NIL) has recently emerged as a powerful patterning tool capable of producing nanoscale patterns in a variety of materials[11−18] and, as such, provides new directions for studies of confinement effects on crystallization. A schematic of the nanoimprint process is shown in Figure 1. Bulk semicrystalline polymers typically exhibit a spherulitic morphology, consisting of lamellae radiating from a central nucleation site. These crystalline structures span a range of length scales, from angstroms for the unit cell of the crystal to millimeters for the spherulitic superstructure. Nanoscale patterning clearly has the potential to influence the crystallization process at several length scales, affecting growth of individual lamellae as well as the development of the larger spherulitic morphologies.
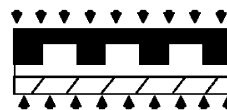
Here we present the effects of patterning via nanoimprint lithography on the crystal morphology of poly(ethylene oxide) (PEO). PEO is an ideal model system because its crystallization behavior has been extensively studied and is well-understood.[19−40] PEO has a low melting temperature and simple chain architecture and forms large spherulites. The crystal lamellae in PEO are on the order of 10 nm thick and can extend for several microns in the lateral directions. In films thicker than 300 nm, spherulitic morphologies are observed and the lamellae usually have an edge-on orientation. In thinner films, the lamellae tend to adopt a flat-on orientation, with their fold surfaces parallel to the substrate.[33,36] As the initial film thickness nears the preferred lamellar thickness, dense-branched morphologies (DBM) are often reported, which are suggested to result from a depletion zone near the growth front.[3]

The nanoimprint mold used in this study consists of parallel line-grating patterns with a periodicity of 400 nm etched into a silicon oxide substrate. The cross section of the lines is approximately trapezoidal, with an average line width of 160 nm, an average line height of 350 nm, and an average sidewall angle of 5° (the sidewall angle is the deviation from a rectangle; 0° would be a rectangle). The mold is treated with a fluorinated self-assembled monolayer (SAM) of tridecafluoro-1,1,2,2-tetrahydrooctyltrichlorosilane to facilitate release of the PEO patterns. PEO films (molar mass ≈ 100 000 g/mol) are spun-

* To whom correspondence should be addressed. E-mail: christopher.soles@nist.gov.
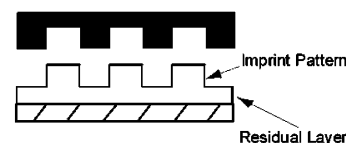† National Research Council Postdoctoral Associate.

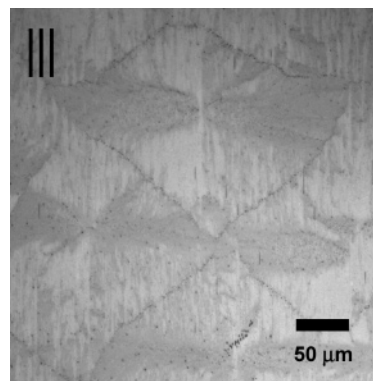**Figure 1.** Schematic of the nanoimprint process.

Figure 2. Optical micrograph of a nanoimprinted PEO film with a spherulitic morphology. The direction of the imprint lines is indicated in the upper left.

cast from 1,2-dichloroethane onto silicon wafers and dried for 2 h at 50 °C to produce a 230 nm thick film. Using a Nanonex NX 2000 imprint tool,[41] the samples are placed under vacuum and imprinted in the melt state at 75 °C for 1 min at 3450 kPa. The samples are crystallized by cooling slowly in the imprint mold to room temperature before releasing the pressure and separating the mold from the sample.

An optical micrograph of an imprinted PEO sample is shown in Figure 2, with a set of three vertical lines indicating the orientation of the grating. AFM scratch tests reveal that the imprinted lines are ∼350 nm tall sitting on a 35 nm thick residual layer. Despite the fact that the continuous portion of the film between the lines is only 35 nm thick, a bulklike spherulitic morphology is observed. This result is surprising given that DBM is normally observed in planar 35 nm thick films.[34] Since the DBM morphology has been claimed to result from a depletion zone at the growth front, we suspect that the molten PEO in the imprinted lines above the thin residual layer acts as a "reservoir" of crystallizable material that feeds the crystallization front. This process facilitates the development of a three-dimensional bulklike spherulite by allowing "communication" through the continuous residual layer and growth of the spherulite into the thick, but discontinuous, patterned region. It is also striking that the radial growth of the spherulites does not appear to be significantly perturbed by the presence
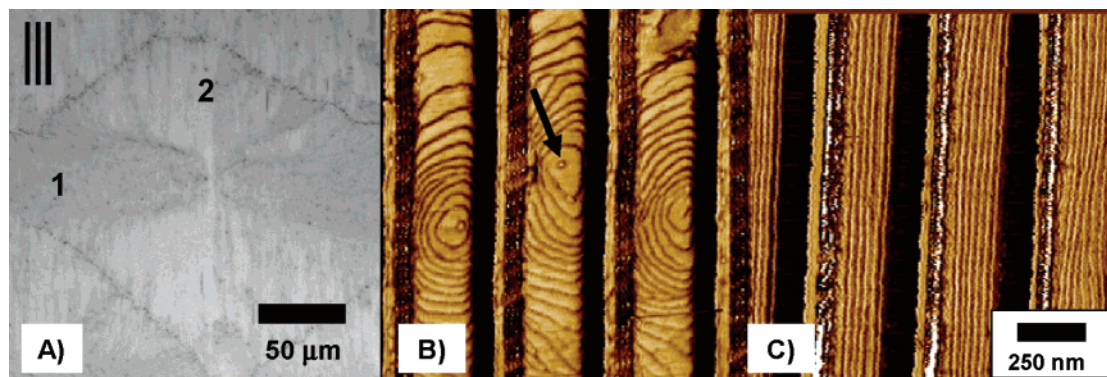
Figure 3. (a) Optical micrograph of nanoimprinted PEO. (b, c) AFM phase micrographs showing the crystal morphology in 240 nm wide imprinted lines with lamellae oriented (b) perpendicular (region 1) and (c) parallel (region 2) to the imprinted lines.
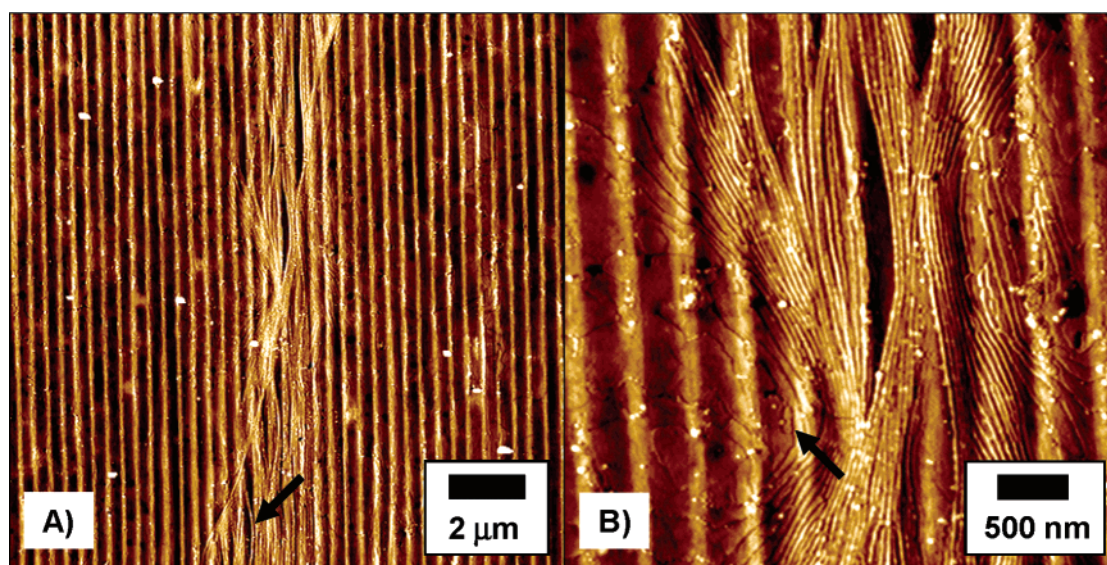

Figure 4. (a) Atomic force height micrograph showing the morphology in the residual layer. (b) Higher resolution micrograph of the spherulite center.

of the imprint lines. We initially anticipated that preferential growth along the direction of the imprinted lines would lead to highly elongated or asymmetric spherulites. Analogous biasing of spherulite formation has been observed for crystallization of poly(ethylene terephthalate) confined between glass fibers,[42] PEO fibers confined in epoxy,[43] and directionally solidified PEO spherulites.[44] We are currently investigating spherulitic growth in films cast directly on the imprint mold to elucidate the influence of the channels on spherulite formation. In the present case, however, the evolution of the macroscopic crystallization morphology is evidently unaffected by the imprinting process and confinement in channels.

To explore these intriguing observations in greater detail, atomic force microscopy (AFM) was used to explore the crystal morphology within the different regions of the spherulite. The optical micrograph in Figure 3a shows a single spherulite with the three vertical lines used to indicate the direction of the imprinted channels. Regions labeled "1" and "2" near the periphery of the spherulite correspond to locations where the primary growth direction of the spherulite is perpendicular and parallel to the imprinted lines, respectively. Figure 3b is a typical AFM micrograph from region 1 showing a flat-on orientation of the lamellae. A large number of screw dislocations are observed (arrow in Figure 3b), with the lamellar steps growing from the dislocation axis. It is important to note that the steps are elongated in the direction parallel to the imprinted line, indicating that the growth direction *within* the imprinted line is orthogonal

to the primary spherulite growth direction. This situation differs from previous reports where crystallization of poly(vinylidene fluoride) (PVDF) in similar nanoimprinted lines was evidently unaffected by the presence of the mold,[18] indicating that the effect of imprinting can be material dependent. We suspect that the preferred orientation of the lamellae relative to the substrate (flat-on in PEO vs edge-on in PVDF) is largely responsible for this difference. It should also be pointed out that the steps around the screw dislocations are often asymmetric, suggesting a tilting of the lamellae in the channel (see Supporting Information). A small amount of tilt is reasonable given that the height of the features is approximately the same as the thickness where lamellae in nonpatterned PEO films tend to lose their flat-on orientation with respect to the substrate.[33,36]

In region 2, where the primary spherulite growth direction is parallel to the imprinted lines, the lamellae are also elongated along the channel direction, as shown in Figure 3c. The terraced morphology results from a tilting of the lamellar stacks (see Supporting Information). Long periods of uninterrupted growth are apparent, suggesting that the mold walls "shield" these lamellar stacks from competition with other lamellae. In contrast to region 1, there are very few screw dislocations at the film surface. In this case, the mold walls are appropriately situated to prevent the screw dislocation from reaching the film surface. As a screw dislocation propagates up from the residual layer to the upper surface, the tilt of the screw dislocation axis may cause the screw dislocation to intersect the edge of the pattern.

The AFM images in Figure 3 reveal the crystal morphology at the top of the imprinted lines but do not provide further insight into how the bulklike spherulitic morphology develops over the length scales of many microns in the discontinuous patterned film. To resolve this issue, we examined the morphology in the residual layer by imprinting a PEO film with a mold that was not treated with the low surface energy release coating.[45] In this case, the imprinted film sticks to the mold upon separation from the substrate, revealing the backside of the residual layer. Parts a and b of Figure 4 are AFM micrographs of the residual layer that was in contact with the flat silicon substrate, revealing a "sheaf" structure that is typically found at the spherulite nucleus (arrow in Figure 4b). In the center of the spherulite, a number of edge-on lamellae are observed that grow parallel to the imprint channels, while flat-on lamellae are observed in the other directions. Some edge-on lamellae are able to grow in other directions, but they eventually either stop growing or reorient themselves along the grating direction (arrow in Figure 4a). These results suggest that the lamellar orientation (flat-on vs edge-on) is determined in the early stages of crystallization and that this orientation is maintained during the crystallization process until the lamellae are either overtaken by lamellae growing with a preferred orientation or until the confining walls force them to find a less resistive path for sustained growth (parallel to the channels).

In summary, crystallization of nanoimprinted PEO was found to be significantly affected by the geometric constraints imposed by the mold. Spherulites were observed even when the residual layer was only ≈35 nm thick. Despite the presence of these spherulitic superstructures, the imprint channels were found to play a large role in directing crystal growth. The lamellae elongate along the direction of the imprint channels even when the spherulite growth direction was perpendicular to the channels. The flat-on orientation of the lamellae in the present study is believed to be responsible for these observations. In addition, the early stages of crystal growth were shown to be critical for determining the lamellar orientation and lamellae with unfavorable orientations either stop growing or reorient themselves in a more preferred direction.

Supporting Information Available: Schematic representations of lamellae in the perpendicular and parallel orientations. This material is available free of charge via the Internet at http://pubs.acs.org.

References and Notes

(1) Despotopoulou, M. M.; Frank, C. W.; Miller, R. D.; Rabolt, J. F. *Macromolecules* **1996**, *29*, 5797−5804.
(2) Sakai, Y.; Imai, M.; Kaji, K.; Tsuji, M. *Macromolecules* **1996**, *29*, 8830−8834.
(3) Taguchi, K.; Miyaji, H.; Izumi, K.; Hoshino, A.; Miyamoto, Y.; Kokawa, R. *Polymer* **2001**, *42*, 7443−7447.
(4) Zhang, F.; Liu, J.; Huang, H.; Du, B.; He, T. *Eur. Phys. J. E* **2002**, *8*, 289−297.
(5) Ferreiro, V.; Douglas, J. F.; Warren, J. A.; Karim, A. *Phys. Rev. E* **2002**, *65*, 0428021−0428024.
(6) Beers, K. L.; Douglas, J. F.; Amis, E. J.; Karim, A. *Langmuir* **2003**, *19*, 3935−3940.
(7) Mareau, V. H.; Prud'homme, R. E. *Macromolecules* **2003**, *36*, 675−684.
(8) Mareau, V. H.; Prud'homme, R. E. *Polymer* **2005**, *46*, 7255−7265.
(9) Steinhart, M.; Göring, P.; Dernaika, H.; Prabhukaran, M.; Gösele, U.; Hempel, E.; Thurn-Albrecht, T. *Phys. Rev. Lett.* **2006**, *97*, 0278011−0278014.
(10) Okerberg, B. C.; Marand, H. *J. Mater. Sci.* Online First: http://dx.doi.org/10.1007/s10853-006-0471-3.
(11) Chou, S. Y.; Krauss, P. R. *Microelectron. Eng.* **1997**, *35*, 237−240.
(12) Chou, S. Y.; Krauss, P. R.; Zhang, W.; Guo, L.; Zhuang, L. *J. Vac. Sci. Technol., B* **1997**, *15*, 2897−2904.
(13) Chou, S. Y.; Keimel, C.; Gu, J. *Nature (London)* **2002**, *417*, 835−837.
(14) Ohtake, T.; Nakamatsu, K.; Matsui, S.; Tabata, H.; Kawai, T. *J. Vac. Sci. Technol., B* **2004**, *22*, 3275−3278.
(15) Firestone, K. A.; Reid, P.; Lawson, R.; Jang, S.; Dalton, L. R. *Inorg. Chim. Acta* **2004**, *357*, 3957−3966.
(16) Guo, L. J.; Cheng, X.; Chao, C. Y. *J. Mod. Opt.* **2002**, *49*, 663−673.
(17) Stewart, M. D.; Wilson, C. G. *MRS Bull.* **2005**, *30*, 947−951.
(18) Hu, Z.; Baralia, G.; Bayot, V.; Gohy, J. F.; Jonas, A. M. *Nano Lett.* **2005**, *5*, 1738−1743.
(19) Price, F. P.; Kilb, R. W. *J. Polym. Sci.* **1962**, *57*, 395−403.
(20) Geil, P. H. *Polymer Single Crystals*; Wiley-Interscience: New York, 1963.
(21) Kovacs, A. J.; Gonthier, A.; Straupe, C. J. *J. Polym. Sci. Symp.* **1975**, *50*, 283−325.
(22) Maclaine, J. Q. G.; Booth, C. *Polymer* **1975**, *16*, 680−684.
(23) Galeski, A.; Kryszewski, M. *J. Polym. Sci., Polym. Phys.* **1976**, *14*, 181−186.
(24) Mihailov, M.; Nedkov, E.; Goshev, I. *J. Macromol. Sci., Part B: Phys.* **1978**, *B15*, 313−328.
(25) Allen, R. C.; Mandelkern, L. *J. Polym. Sci., Polym. Phys.* **1982**, *20*, 1465−1484.
(26) Cheng, S. Z. D.; Bu, H. S.; Wunderlich, B. *J. Polym. Sci., Part B: Polym. Phys.* **1988**, *26*, 1947−1964.
(27) Cheng, S. Z. D.; Chen, J.; Janimak, J. J. *Polymer* **1990**, *31*, 1018−1024.
(28) Schultz, J. M.; Miles, M. J. *J. Polym. Sci., Part B: Polym. Phys.* **1998**, *36*, 2311−2325.
(29) Pearce, R.; Vancso, G. J. *Polymer* **1998**, *39*, 1237−1242.
(30) Reiter, G.; Sommer, J. *Phys. Rev. Lett.* **1998**, *80*, 3771−3774.
(31) Reiter, G.; Sommer, J. *J. Chem. Phys.* **2000**, *112*, 4376−4383.
(32) Dalnoki-Veress, K.; Forrest, J. A.; Massa, M. V.; Pratt, A.; Williams, A. *J. Polym. Sci., Part B: Polym. Phys.* **2001**, *39*, 2615−2621.
(33) Schönherr, H.; Waymouth, R. M.; Hawker, C. J.; Frank, C. W. *Polym. Mater. Sci. Eng.* **2001**, *84*, 453−454.
(34) Massa, M. V.; Dalnoki-Veress, K.; Forrest, J. A. *Eur. Phys. J. E* **2003**, *11*, 191−198.
(35) Kurimoto, R.; Kawaguchi, A. *J. Macromol. Sci., Part B: Phys.* **2003**, *B42*, 441−453.
(36) Schönherr, H.; Frank, C. W. *Macromolecules* **2003**, *36*, 1188−1198.
(37) Schönherr, H.; Frank, C. W. *Macromolecules* **2003**, *36*, 1199−1208.
(38) Ok, S.; Demirel, A. L. *J. Macromol. Sci., Part B: Phys.* **2003**, *B42*, 611−620.
(39) Hobbs, J. K.; Vasilev, C.; Humphris, A. D. L. *Polymer* **2005**, *46*, 10226−10236.
(40) Zhai, X.; Wang, W.; Zhang, G.; He, B. *Macromolecules* **2006**, *39*, 324−329.
(41) Certain equipment, instruments, or materials are identified in this paper in order to adequately specify the experimental details. Such identification does not imply recommendation by the National Institute of Standards and Technology nor does it imply the materials are necessarily the best available for the purpose.
(42) Lhymn, C.; Schultz, J. M. *Polym. Compos.* **1985**, *6*, 87−92.
(43) Schultz, J. M. *J. Polym. Sci., Part B: Polym. Phys.* **1992**, *30*, 785−786.
(44) Lovinger, A. J.; Gryte, C. C. *Macromolecules* **1976**, *9*, 247−253.
(45) Preliminary studies of films cast on untreated molds indicate that the crystal morphology is unaffected by presence of the SAM layer.